Heat-Transfer Characteristics in Annuli with Blowing or Suction at the Walls

Amir Faghri*
Wright State University, Dayton, Ohio

Numerical solutions were obtained for thermally and hydrodynamically developing laminar flow in annular passages with blowing and suction at the walls. Two separate thermal boundary conditions at the walls were studied: arbitrarily prescribed constant temperatures and constant heat fluxes at each wall. Cases involving blowing, suction, and impermeable walls were considered. Assuming that the properties of the fluid are constant and the injection or extraction velocities at the walls are uniform, the results were obtained in the form of pressure drops and Nusselt numbers. The results are presented for several inner-to-outer tube radius ratios, Prandtl numbers, and injection and extraction Reynolds numbers at the walls.

Nomenclature

A = surface area
$A_{j,k}$ = coefficient, Eq. (16)
$a_{j,k}$ = coefficient, Eq. (19)
$B_{j,k}$ = coefficient, Eq. (16)
$b_{j,k}$ = coefficient, Eq. (19)
$C_{j,k}$ = coefficient, Eq. (16)
$c_{j,k}$ = coefficient, Eq. (19)
C_p = specific heat of the fluid
D_h = hydraulic diameter, $2(R_o - R_i)$
D_j = coefficient, Eq. (16)
$d_{j,k}$ = coefficient, Eq. (19)
$E_{j,k}$ = coefficient, Eq. (16)
h = convective heat-transfer coefficient
K = ratio of the inner radius to the outer radius of the annulus, R_i/R_o
k = thermal conductivity of the fluid
Nu = Nusselt number, $h\,D_h/k$
P^+ = dimensionless pressure, $(P - P_e)/\rho\,w_e^2$
P = pressure
Pr = Prandtl number, $\mu\,C_p/k$
Q = heat-transfer rate
r = radial direction
r^+ = dimensionless radial distance, r/R_o
Re_i = radial Reynolds number at the inner wall, $R_i\,v_i/\nu$
Re_o = radial Reynolds number at the outer wall, $R_o\,v_o/\nu$
R_i = inner radius of the annulus
R_o = outer radius of the annulus
T = temperature
v = radial component of velocity
v^+ = dimensionless radial velocity, $R_o\,v/\nu$
w = axial component of velocity
w^+ = dimensionless axial velocity, w/w_e
z = axial direction
z^+ = dimensionless axial distance, $\nu z/R_o^2\,w_e$
$\theta_\ell^{(1)}$ = dimensionless temperature for the fundamental solution of the first kind, $(T - T_e)/(T_\ell - T_e)$
$\theta_\ell^{(2)}$ = dimensionless temperature for the fundamental solution of the second kind, $[k/(R_o\,Q_\ell/A_\ell)]\,(T - T_e)$
$\theta_{m\ell}$ = dimensionless mean temperature
μ = absolute viscosity of the fluid
ν = kinematic viscosity of the fluid
ρ = density of the fluid

Superscripts

$+$ = dimensionless variable
(1) = fundamental solution of the first kind
(2) = fundamental solution of the second kind

Subscripts

e = entrance to the annulus
i = inner wall
j = grid location in the z direction
k = grid location in the r direction
ℓ = dummy subscript: i, o
m = mixed mean
o = outer wall

Introduction

THE annulus represents a common geometry employed in a variety of heat-transfer equipment ranging from simple heat exchangers to complicated nuclear reactors. Although there have been numerous studies of both laminar and turbulent heat transfer in annuli,[1-3] all of these efforts have been restricted to the case of impermeable walls.

Consideration of the available results for other types of laminar internal flows indicates that blowing or suction at the boundary can have a significant effect on all of the transfer coefficients. It is also to be expected that injection or extraction at the walls will have a distinct effect on the heat-transfer characteristics of laminar annular flows. Heat transfer in laminar flows with blowing or suction at the walls for the limiting forms of the annulus (i.e., the circular tube and the parallel plane channel) has received considerable attention in the past.[4-10] Recently, the author has presented the hydrodynamic problem for uniform blowing and suction at the walls of annuli with zero and parabolic entry velocity profiles for the analysis of annular heat pipes.[11] A search of the literature disclosed no prior work for laminar, forced convective heat and mass transfer in annular passages with porous walls.

The subject of fluid flow in annuli with porous walls has received attention recently because of applications to the area of the annular heat pipe.[11-14] The annular heat pipe consists of two concentric pipes of unequal diameters attached by end caps that form an annular vapor space between the two pipes. Wick structures can be placed on both the inner surface of the outer pipe and the outer surface of the inner pipe. The space inside the inner pipe is open to the surroundings. An increase in performance is expected as a result of the increase in surface area exposed for the transfer of heat into and out of the pipe,

Received Sept. 26, 1988; revision received April 4, 1989.

*Professor, Mechanical Systems Engineering. Senior Member AIAA.

and the increase in capillary pressure due to the increase in the wick surface area inside the pipe.

The present study is restricted to laminar incompressible flow with the simultaneous development of the velocity and temperature fields. The thermal boundary conditions considered for this problem correspond to the fundamental solutions of the first and second kind as presented by Reynolds et al.[1] for impermeable walls. The fundamental solution of the first kind is when one wall is held at the inlet temperature and the opposite wall experiences a step temperature. With the results from the two cases where each wall individually undergoes a step temperature, the superposition approach can be used, as shown in a latter section, to determine the heat flux for constant wall temperatures arbitrarily prescribed at each wall. The fundamental solution of the second kind refers to the thermal boundary condition when one wall is insulated and the opposite wall experiences a step heat flux. The superposition principle can also be used in a manner similar to the fundamental solution of the first kind to determine the Nusselt numbers for the general case when both walls are heated with arbitrary heat fluxes.

Upon assuming that the properties of the fluid are constant and the injection or extraction velocities at the walls are uniform, the heat-transfer characteristics for flow in annuli with porous walls with the fundamental solutions of the first and second kind as the thermal boundary conditions are obtained. The results are presented in the form of pressure drops, Nusselt numbers, and nondimensional mean temperatures over a range of injection and extraction radial Reynolds numbers for several inner-to-outer radius ratios and Prandtl numbers.

Analysis

The fluid flow is considered to be laminar, incompressible, and steady with the properties of the fluid being constant. The boundary-layer assumptions are imposed which neglect the transverse pressure gradient and longitudinal diffusion. It should be noted that the boundary-layer assumption is not valid for low axial-flow Reynolds numbers and substantial injection/suction. The fluid that enters or leaves through the walls is assumed to be at the same temperature as the wall through which it enters or exits and is the same fluid as in the main annular flow. The cylindrical coordinate system used for the development of the problem is shown in Fig. 1.

The governing equations that describe this problem are the conservation of mass, axial momentum, and energy, where upon nondimensionalization are

$$r^+ \frac{\partial w^+}{\partial z^+} + \frac{\partial (r^+ v^+)}{\partial r^+} = 0 \tag{1}$$

$$w^+ \frac{\partial w^+}{\partial z^+} + v^+ \frac{\partial w^+}{\partial r^+} = -\frac{\partial P^+}{\partial z^+} + \frac{\partial^2 w^+}{\partial r^{+2}} + \frac{1}{r^+}\frac{\partial w^+}{\partial r^+} \tag{2}$$

$$w^+ \frac{\partial \theta}{\partial z^+} + v^+ \frac{\partial \theta}{\partial r^+} = \frac{1}{Pr}\left[\frac{\partial^2 \theta}{\partial r^{+2}} + \frac{1}{r^+}\frac{\partial \theta}{\partial r^+}\right] \tag{3}$$

Since the thermal boundary conditions for the two fundamental solutions are different, the energy equation will be nondimensionalized separately for each case with the following definitions:

Fundamental solution of the first kind:

$$\theta_\ell^{(1)} = (T - T_e)/(T_\ell - T_e)$$

where $\ell \equiv i$ when the inner wall is heated and $\ell \equiv o$ when the outer wall is heated.

Fundamental solution of the second kind:

$$\theta_\ell^{(2)} = \frac{k}{R_o Q_\ell / A_\ell}(T - T_e)$$

where the subscript defines which wall is being heated as previously stated.

The point $z^+ = 0$ was used to designate the entrance to the annulus, where a uniform velocity and temperature is assumed to exist. Equation (3) is linear and homogeneous and the sum of multiples of any solutions will also be a solution, which means that one can obtain rather complex solutions by adding together a variety of simpler solutions.

The hydrodynamic boundary conditions for the case of a uniform inlet velocity profile and constant injection or extraction velocities at the walls are as follows:

$$w^+(0, r^+) = 1, \quad w^+(z^+, K) = w^+(z^+, 1) = 0$$

$$v^+(z^+, K) = \frac{Re_i}{K}, \quad v^+(z^+, 1) = Re_o, \quad P^+(0, r^+) = 0 \tag{4}$$

The sign convention for injection and extraction is given by the following definitions:

Injection:	$Re_i > 0,\ Re_o < 0$
Extraction:	$Re_i < 0,\ Re_o > 0$
Impermeable wall:	$Re_i = Re_o = 0$

A negative transverse velocity at the outer surface constitutes injection, whereas the reverse is true at the inner surface. For extraction, the outer velocity is positive, whereas it is negative at the inner surface.

The thermal boundary conditions for the fundamental solutions of the first and second kind will now be discussed.

Fundamental Solution of the First Kind

Consider the general thermal boundary conditions:

$$T = T_e, \qquad \text{everywhere for } z^+ \le 0 \tag{5a}$$

$$T = T_i, \qquad r^+ = K,\ z^+ > 0 \tag{5b}$$

$$T = T_o, \qquad r^+ = 1,\ z^+ > 0 \tag{5c}$$

Let $\theta_o^{(1)}$ be the solution to Eq. (3) subject to the dimensionless boundary conditions:

$$\theta_o^{(1)} = 0, \qquad \begin{cases} \text{(a) everywhere for } z^+ \le 0 \\ \text{(b) } r^+ = K,\ z^+ > 0 \end{cases} \tag{6a}$$

$$\theta_o^{(1)} = 1, \qquad r^+ = 1,\ z^+ > 0 \tag{6b}$$

which represents the solution corresponding to a step temperature on the outer wall, with the inner wall maintained at the inlet temperature. Let $\theta_i^{(1)}$ be the solution to Eq. (3) subject to

$$\theta_i^{(1)} = 0, \qquad \begin{cases} \text{(a) everywhere for } z^+ \le 0 \\ \text{(b) } r^+ = 1,\ z^+ > 0 \end{cases} \tag{7a}$$

$$\theta_i^{(1)} = 1, \qquad r^+ = K,\ z^+ > 0 \tag{7b}$$

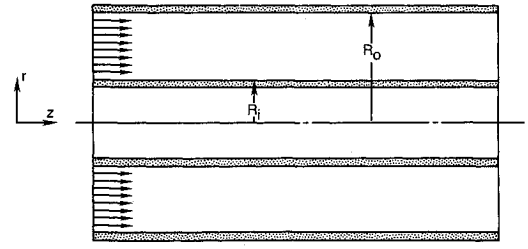

Fig. 1 Coordinate system for the annulus with uniform porous walls.

which represents the solution corresponding to a step temperature on the inner wall, with the outer wall maintained at the inlet temperature. The solution of Eq. (3) satisfying the general thermal boundary conditions given in Eq. (5) is

$$T(r^+, z^+) = (T_o - T_e)\,\theta_o^{(1)}(r^+, z^+) + (T_i - T_e)\,\theta_i^{(1)}(r^+, z^+) + T_e \tag{8}$$

With the temperatures at the inner and outer walls prescribed, the Nusselt numbers for the inner and outer walls based on the hydraulic diameter for the two cases are defined in terms of the dimensionless heat fluxes at the walls by the following relations:

$$Nu_{oo}^{(1)} = \frac{2(1-K)\left[\frac{d\theta_o^{(1)}}{dr^+}\right]_{r^+=1}}{1-\theta_{mo}^{(1)}}, \qquad Nu_{io}^{(1)} = \frac{2(1-K)\left[\frac{d\theta_o^{(1)}}{dr^+}\right]_{r^+=K}}{\theta_{mo}^{(1)}} \tag{9a}$$

$$Nu_{ii}^{(1)} = \frac{-2(1-K)\left[\frac{d\theta_i^{(1)}}{dr^+}\right]_{r^+=K}}{1-\theta_{mi}^{(1)}}, \qquad Nu_{oi}^{(1)} = \frac{-2(1-K)\left[\frac{d\theta_i^{(1)}}{dr^+}\right]_{r^+=1}}{\theta_{mi}^{(1)}} \tag{9b}$$

where

$$\theta_{mi}^{(1)} = \frac{2}{(1-K^2)w_m^+}\int_K^1 w^+\theta_i^{(1)} r^+\,dr^+$$

represents the dimensionless mixed-mean temperature. In Eq. (9), the first subscript on the Nusselt number refers to the wall at which the heat flux is evaluated, and the second subscript refers to the wall that is being heated. For example, $Nu_{io}^{(1)}$ refers to the Nusselt number at the inner wall when the outer wall is being heated for the fundamental solution of the first kind.

Fundamental Solution of the Second Kind

Consider the general thermal boundary conditions:

$$T = T_e, \qquad \text{everywhere for } z^+ \le 0 \tag{10a}$$

$$-k\frac{dT}{dr} = Q_i/A_i, \qquad r^+ = K,\ z^+ > 0 \tag{10b}$$

$$-k\frac{dT}{dr} = -Q_o/A_o, \qquad r^+ = 1,\ z^+ > 0 \tag{10c}$$

Let $\theta_o^{(2)}$ be the solution to Eq. (3) subject to the following dimensionless boundary conditions:

$$\theta_o^{(2)} = 0, \qquad \text{everywhere for } z^+ \le 0 \tag{11a}$$

$$\frac{\partial\theta_o^{(2)}}{\partial r^+} = 0, \qquad r^+ = K,\ z^+ > 0 \tag{11b}$$

$$\frac{\partial\theta_o^{(2)}}{\partial r^+} = 1, \qquad r^+ = 1,\ z^+ > 0 \tag{11c}$$

which represents the solution to a step heat flux through the outer wall with the inner wall insulated. Similarly, let $\theta_i^{(2)}$ be the solution to Eq. (3) subject to

$$\theta_i^{(2)} = 0, \qquad \text{everywhere for } z^+ \le 0 \tag{12a}$$

$$\frac{\partial\theta_i^{(2)}}{\partial r^+} = -1, \qquad r^+ = K,\ z^+ > 0 \tag{12b}$$

$$\frac{\partial\theta_i^{(2)}}{\partial r^+} = 0, \qquad r^+ = 1,\ z^+ > 0 \tag{12c}$$

which represents the solution to a step heat flux through the inner wall with the outer wall insulated.

At any point along the annulus, the local Nusselt number on the active wall is defined based on the mixed-mean temperature and the hydraulic diameter. The following expressions are the local Nusselt numbers for the two cases.

$$Nu_{oo}^{(2)} = \frac{2(1-K)}{(\theta_{oo}^{(2)} - \theta_{mo}^{(2)})} \tag{13a}$$

$$Nu_{ii}^{(2)} = \frac{2(1-K)}{(\theta_{ii}^{(2)} - \theta_{mi}^{(2)})} \tag{13b}$$

where

$$\theta_{mi}^{(2)} = \frac{2}{(1-K^2)w_m^+}\int_K^1 w^+\theta_i^{(2)} r^+\,dr^+$$

In Eq. (13), the first subscript on the dimensionless temperatures and the Nusselt numbers refers to the wall at which the variable is being evaluated, and the second subscript refers to the wall that is being heated. By superposition, the Nusselt number at each wall for the general case when both walls are heated with arbitrary heat fluxes is given by the following equations:

$$Nu_i = \frac{2(1-K)Q_i/A_i}{Q_o/A_o(\theta_{io}^{(2)} - \theta_{mo}^{(2)}) + Q_i/A_i(\theta_{ii}^{(2)} - \theta_{mi}^{(2)})} \tag{14}$$

$$Nu_o = \frac{2(1-K)Q_o/A_o}{Q_o/A_o(\theta_{oo}^{(2)} - \theta_{mo}^{(2)}) + Q_i/A_i(\theta_{oi}^{(2)} - \theta_{mi}^{(2)})} \tag{15}$$

where Q_i/A_i and Q_o/A_o are the prescribed heat fluxes at the inner and outer walls, respectively.

Numerical Solution Procedure

The solution procedure used for the dimensionless mass and momentum equations [Eqs. (1 and 2)] is similar to the procedure discussed in detail in the paper by Faghri[11] in conjunction with the prediction of the vapor pressure drop in a concentric annular heat pipe. The main difference is that the zero axial inlet velocity and the fully developed profile were used rather than the uniform inlet velocity needed in this problem. The solution of the energy equation is more straightforward than the momentum equation due to the fact that three unknowns appear in each equation, and therefore one can use the simplified Gaussian-elimination method. An implicit marching finite-difference method is used to solve Eqs. (1 and 2). The resulting finite-difference equation for Eq. (2) using a backward difference in z^+, a central difference in r^+, and rearranging yields

$$A_{j,k}w_{j+1,k-1}^+ + B_{j,k}w_{j+1,k}^+ + C_{j,k}w_{j+1,k+1}^+ + D_j P_{j+1}^+ = E_{j,k} \tag{16}$$

where the explicit formulas for $A_{j,k}$, $B_{j,k}$, $C_{j,k}$, D_j, and $E_{j,k}$ are given by Faghri.[11] It should be noted that in Eq. (2), v^+ is evaluated at the node (j,k) and it is contained in $A_{j,k}$ and $C_{j,k}$ when it is presented in the form of Eq. (16). The details are given in Ref. 11.

In finite-difference form, Eq. (1) may be written as

$$r_k^+ \frac{w_{j+1,k}^+ - w_{j,k}^+}{2\Delta z^+} + r_{k+1}^+ \frac{w_{j+1,k+1}^+ - w_{j,k+1}^+}{2\Delta z^+} + \frac{v_{j+1,k+1}^+ r_{k+1}^+ - v_{j+1,k}^+ r_k^+}{\Delta r^+} = 0 \tag{17}$$

By summing Eq. (17) for $k = 1,\ldots,n$, the following equation may be obtained:

$$\sum_{k=2}^{n} r_k^+ w_{j+1,k}^+ - \sum_{k=2}^{n} r_k^+ w_{j,k}^+ + \frac{\Delta z^+}{\Delta r^+} r_n^+ Re_o - \frac{\Delta z^+}{\Delta r^+} r_1^+ \frac{Re_i}{K} = 0 \tag{18}$$

A forward difference is used to approximate $\partial\theta/\partial z^+$, and a central difference is used to approximate $\partial\theta/\partial r^+$. The finite-difference representation of Eq. (3) is rearranged in order to obtain the following expression:

$$a_{j,k}\theta_{j+1,k-1} + b_{j,k}\theta_{j+1,k} + c_{j,k}\theta_{j+1,k+1} = d_{j,k} \tag{19}$$

where the explicit formulas for $a_{j,k}$, $b_{j,k}$, $c_{j,k}$, and $d_{j,k}$ are obtained in a similar manner as for the momentum equation. Equations (16) and (18) provide $(n + 1)$ linear equations with $(n + 1)$ unknowns $w_{j+1,k}^+$ and P_{j+1}^+. After these equations have been solved using the Gaussian-elimination method, Eq. (17) is solved for $v_{j+1,k}^+$. The simplified Gaussian-elimination procedure is used to solve for $\theta_{j,k}$ by substituting the known quantities $w_{j+1,k}^+$ and $v_{j+1,k}^+$ into Eq. (19).

The process is repeated along the z^+ direction by marching to the desired final location. A total of 200 grids in the radial direction were needed. It was found necessary to use grid meshes as small as $\Delta z^+ = 10^{-5}$ near the inlet in the axial direction and gradually increasing the mesh size at large z^+. The results in the region very close to the entrance are predictive rather than exact, since the transverse momentum equation has not been used. Therefore, the results very close to the inlet are not reported ($z^+ < 10^{-3}$). All of the results presented in the paper are grid independent.

Results and Discussion

One of the results of primary interest to the present work is the functional relationship between the pressure drop and the injection and extraction Reynolds numbers at the walls, which is presented in Figs. 2-3 for various blowing and suction velocities at the walls for $K = 0.1$ and 0.8, respectively. For comparison, the results for impermeable walls are also plotted for each K value. The present numerical results are limited to the cases of symmetric radial Reynolds numbers at the walls due to the many different combinations of radial Reynolds numbers one can assume for asymmetric cases. For all of the cases of injection and impermeable walls, the pressure drops with increasing z^+ because of the shear stress at the walls. If the suction velocity is low ($Re_i = -1$, $Re_o = 1$), the effect of the shear stress at the walls will be larger than that due to the loss of axial momentum flux and the pressure drops along the annulus. As the suction velocity increases, the pressure first drops and then starts to rise. The initial pressure drop is due to the very high shear stress at the walls associated with a uni-

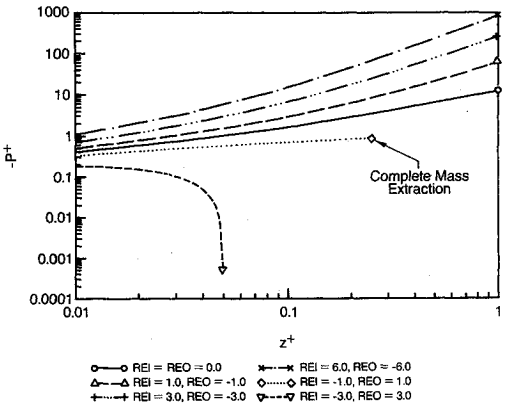

Fig. 2 Nondimensional pressure distribution along the annulus for $K = 0.1$ and different injection and extraction wall Reynolds numbers.

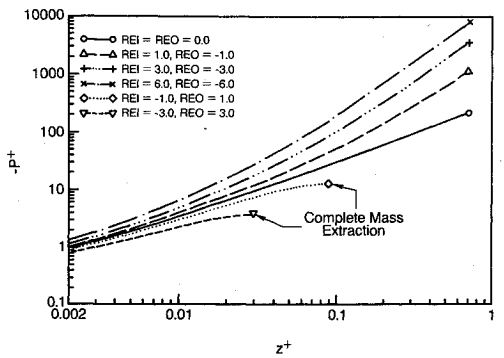

Fig. 3 Nondimensional pressure distribution along the annulus for $K = 0.8$ and different injection and extraction wall Reynolds numbers.

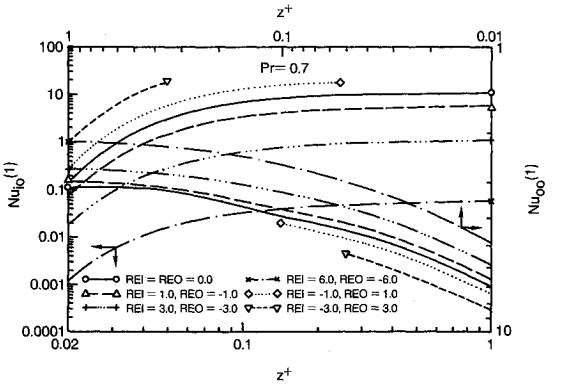

Fig. 4 Axial variation of the inner and outer wall Nusselt numbers for the fundamental solution of the first kind (outer wall heated, $K = 0.1$).

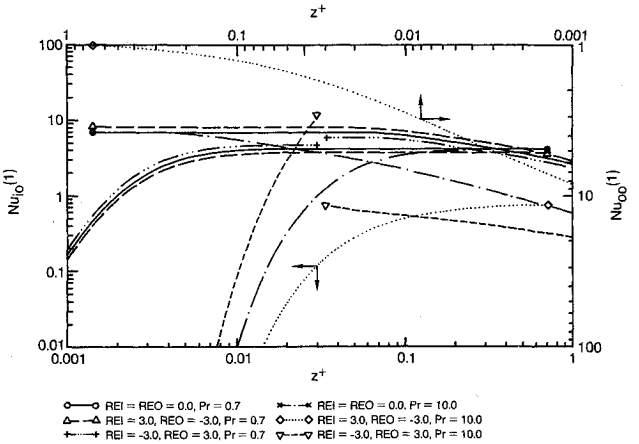

Fig. 5 Axial variation of the inner and outer wall Nusselt numbers for the fundamental solution of the first kind (outer wall heated, $K = 0.8$).

form inlet velocity. Only after the high velocity gradients at the wall have decreased somewhat does the large loss of axial momentum due to suction at the walls begin to have an effect on the pressure, causing it to rise along the annulus.

The behavior of the Nusselt numbers in the entrance region at the inner and outer walls for $K = 0.1$ and 0.8 are given in Figs. 4–7 for the fundamental solution of the first kind. Figures 4–5 present the results of the case when the outer wall is heated, and Figs. 6–7 give the results of the case when the inner wall is heated. All of the results are presented for $Pr = 0.7$ except with $K = 0.8$, which are presented for $Pr = 0.7$ and $Pr = 10$ in Figs. 5 and 7. The dimensionless pressure drops, mean temperatures, and Nusselt numbers for $K = 0.5$ are presented in Table 1 for selected axial distances for the fundamental solution of the first kind. Table 1 provides information on the mean temperature in addition to the Nusselt numbers for the fundamental solution of the first kind, since one needs to know this information to calculate the heat flux for the cases of constant wall temperature.

The Nusselt numbers at the inner wall begin at zero and increase along pipe until uniform values are reached when the outer wall is heated. For the same case, the Nusselt numbers at the outer wall start at high values and decrease until uniform values are reached. An opposite trend is observed for the case when the inner wall is heated as expected. These trends are similar to heat transfer in annuli with impermeable walls as given by Lundberg et al.[2]

For a fixed Prandtl number, the effect of injection is to reduce the Nusselt numbers for both the inner and outer walls and thus the heat transfer for a given wall-to-bulk temperature difference. In the case of extraction, the opposite effect occurs and the Nusselt numbers increase with increasing suction Reynolds numbers at the wall. A similar behavior is observed for heat transfer in porous wall ducts.[4] Because of the decreasing nature of the Nusselt number or temperature gradient at the walls by increasing the injection at the wall, one is able to protect the wall of an annulus from a hot gas or liquid by injecting a relatively cool fluid into the annular flow.

Referring to Figs. 5 and 7, it can be seen that when there is injection or extraction at the walls of the annulus, the Nusselt

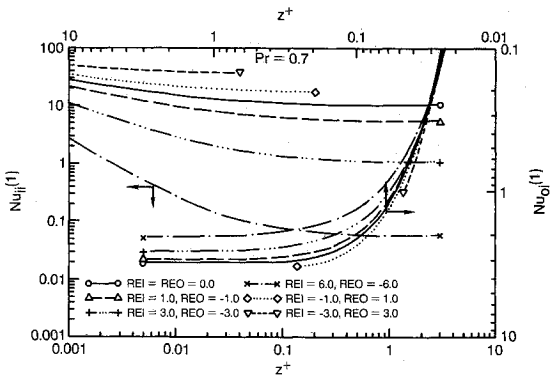

Fig. 6 Axial variation of the inner and outer wall Nusselt numbers for the fundamental solution of the first kind (inner wall heated, $K = 0.1$).

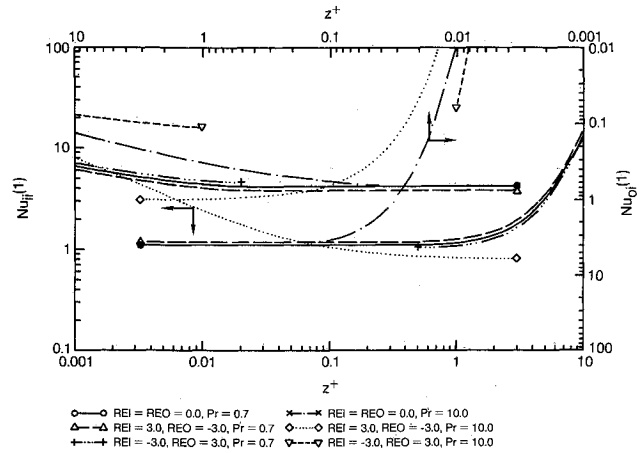

Fig. 7 Axial variation of the inner and outer wall Nusselt numbers for the fundamental solution of the first kind (inner wall heated, $K = 0.8$).

Table 1 Results of the flow and heat-transfer analysis with blowing or suction at the walls of the annulus for the fundamental solution of the first kind ($K = 0.5$, $Pr = 0.7$)

Re_i	Re_o	z^+	P^+	$\theta^{(1)}_{mo}$	$Nu^{(1)}_{io}$	$Nu^{(1)}_{oo}$	$\theta^{(1)}_{mi}$	$Nu^{(1)}_{ii}$	$Nu^{(1)}_{oi}$
0.0	0.0	0.01	−0.8065	0.2630	0.6266	5.189	0.1649	6.580	0.442
		0.05	−2.7130	0.5307	4.3680	3.890	0.3648	5.198	3.169
		0.10	−5.0820	0.5828	4.8190	3.576	0.4042	4.919	3.485
		0.50	−24.030	0.5902	4.8760	3.525	0.4098	4.876	3.525
		1.00	−47.730	0.5902	4.8760	3.525	0.4098	4.876	3.525
1.0	−1.0	0.01	−0.9422	0.2660	0.5213	4.943	0.1702	5.933	0.401
		0.05	−3.7290	0.5183	3.7330	3.701	0.3638	4.630	2.902
		0.10	−7.9260	0.5711	4.1800	3.397	0.4049	4.357	3.233
		0.50	−70.340	0.5846	4.2820	3.307	0.4154	4.282	3.307
		1.00	−220.40	0.5846	4.2820	3.307	0.4154	4.282	3.307
3.0	−3.0	0.01	−1.2360	0.2720	0.3606	4.477	0.1814	4.774	0.332
		0.05	−6.2730	0.4995	2.7000	3.321	0.3660	3.612	2.442
		0.10	−15.630	0.5500	3.0930	3.051	0.4077	3.372	2.775
		0.50	−213.10	0.5727	3.2480	2.910	0.4265	3.253	2.905
		1.00	−766.70	0.5731	3.2500	2.907	0.4268	3.251	2.907
6.0	−6.0	0.01	−1.7350	0.2808	0.2056	3.841	0.1986	3.355	0.252
		0.05	−11.380	0.4814	1.6200	2.783	0.3751	2.398	1.896
		0.10	−32.320	0.5261	1.9040	2.560	0.4155	2.213	2.203
		0.50	−554.90	0.5546	2.0630	2.397	0.4413	2.085	2.372
		1.00	−2094.0	0.5561	2.0710	2.388	0.4427	2.077	2.381
−1.0	1.0	0.01	−0.6783	0.2600	0.7517	5.444	0.1596	7.270	0.488
		0.02	−1.0110	0.3790	2.8860	4.807	0.2451	6.572	1.952
		0.05	−1.8660	0.5460	5.0920	4.071	0.3681	5.800	3.467
		0.08	−2.5470	0.5873	5.4580	3.812	0.3985	5.572	3.711
		0.10	−2.9070	0.5936	5.5100	3.768	0.4032	5.535	3.745
−3.0	3.0	0.01	−0.4445	0.2539	1.0790	5.982	0.1497	8.785	0.596
		0.02	−0.5356	0.3848	4.0560	5.329	0.2400	8.064	2.404
		0.04	−0.6438	0.5499	6.4680	4.611	0.3572	7.290	3.937
		0.05	−0.6723	0.5893	6.8490	4.362	0.3854	7.068	4.175

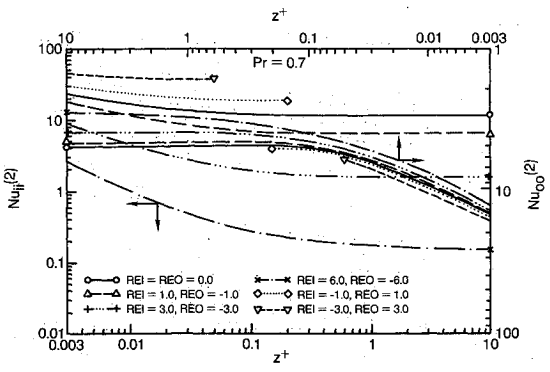

Fig. 8 Axial variation of the inner and outer wall Nusselt numbers for the fundamental solution of the second kind ($K = 0.1$).

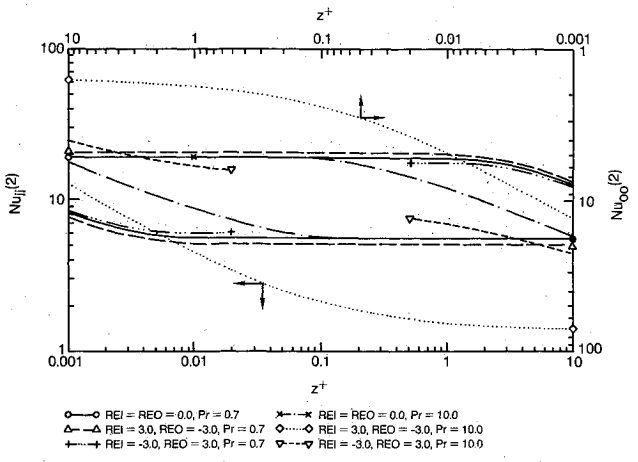

Fig. 9 Axial variation of the inner and outer wall Nusselt numbers for the fundamental solution of the second kind ($K = 0.8$).

numbers are strongly affected by the fluid Prandtl number. This is to be expected because the quantity of heat rejection or addition from the main stream to or from the walls depends greatly on the fluid heat capacity, which is a quantity used to form the Prandtl number. However, it should be noted that the fully developed Nusselt numbers for an impermeable wall annulus are independent of the Prandtl number as in the case of the classical fully developed Graetz problem.[15]

The results of the numerical computations for the fundamental solution of the second kind are presented in Figs. 8-9 for $K = 0.1$ and 0.8. All of the results are presented for $Pr = 0.7$ except the results with $K = 0.8$, which are presented for $Pr = 0.7$ and $Pr = 10$ in Fig. 9. Table 2 provides information on the mixed mean temperature and the Nusselt number for the fundamental solution of the second kind for $K = 0.5$.

Several observations can be made concerning the characteristics of the flow in the present situation. All of the thermal entry Nusselt number curves shown in Figs. 8-9 have the same general shape, which is similar to the results for the fundamental solution of the first kind. As the tube radius ratio increases, the fully developed Nusselt number at the outer wall increases and the fully developed Nusselt number at the inner wall decreases. As would be expected, the temperature profile becomes fully developed in a shorter distance as the radius ratio increases because the thermal boundary layers are closer together and meet in a shorter distance.

When the injection Reynolds numbers are increased, the Nusselt numbers decrease and the thermal entry length is longer. When the extraction Reynolds numbers are increased, it is seen that the Nusselt numbers increase. In comparing the case of constant heat rate with the case of constant surface temperature, it is found that the fully developed Nusselt number is higher for the case of constant heat rate with the same blowing or suction specification, which agrees with the solutions given by Kays and Crawford[15] for circular pipes with impermeable walls and the numerical results given by Doughty and Perkins[7] for parallel porous plates.

Two methods were used to validate the results. First, a comparison was made with the analytical results for impermeable walls with simultaneously developing velocity and temperature fields[3] and hydrodynamically developed laminar flow.[2] The results were in excellent agreement to within 3% for the Nusselt numbers in the thermal entry and fully developed regions for the fundamental solutions of the first and second kinds. Second, an overall energy balance was made for the control volume bounded by $z^+ = 0$, $z^+ = z^+$, $r^+ = K$, and $r^+ = 1$. The conservation of energy requires the following relations for the two cases of the fundamental solution of the first kind:

$$2\frac{K}{Pr}\left[\int_0^{z^+}\left.\frac{d\theta_o^{(1)}}{dr^+}\right|_{r^+=K} dz^+\right] - \frac{2}{Pr}\left[\int_0^{z^+}\left.\frac{d\theta_o^{(1)}}{dr^+}\right|_{r^+=1} dz^+\right] = -\theta_{mo}^{(1)} w_m^+ (1-K^2) - 2\,Re_o\, z^+ \tag{20}$$

$$2\frac{K}{Pr}\left[\int_0^{z^+}\left.\frac{d\theta_i^{(1)}}{dr^+}\right|_{r^+=K} dz^+\right] - \frac{2}{Pr}\left[\int_0^{z^+}\left.\frac{d\theta_i^{(1)}}{dr^+}\right|_{r^+=1} dz^+\right] = -\theta_{mi}^{(1)} w_m^+ (1-K^2) + 2\,Re_i\, z^+ \tag{21}$$

The energy balances for the two cases of the fundamental solution of the second kind results in

$$2\left(\frac{z^+}{Pr} - Re_o\int_0^{z^+}\theta_{oo}^{(2)}\,dz^+ + Re_i\int_0^{z^+}\theta_{io}^{(2)}\,dz^+\right) = w_m^+(1-K^2)\theta_{mo}^{(2)} \tag{22}$$

$$2\left(\frac{K}{Pr}\,z^+ - Re_o\int_0^{z^+}\theta_{oi}^{(2)}\,dz^+ + Re_i\int_0^{z^+}\theta_{ii}^{(2)}\,dz^+\right) = w_m^+(1-K^2)\theta_{mi}^{(2)} \tag{23}$$

The energy balances were within 3% for all of the reported results for the cases considered in this report.

The practical significance of the results for the case of suction lies to the point where all of the fluid has been extracted from the annulus. This requires that

$$(1-K^2) = 2z^+(Re_o - Re_i) \tag{24}$$

The final z^+ for the numerical results with suction is obtained from the above equation. For the case $K = 0.1$ and $Re_i = -3.0$ and $Re_o = 3.0$, the numerical results are terminated when the pressure drop approaches zero, as shown in Fig. 2. There are no such restrictions for the cases with blowing and one can obtain fully developed thermal and hydrodynamic flow results. Hydrodynamically, fully developed flow is defined as the point at which the normalized velocity w^+/w_m^+ becomes insensitive to z^+ past a hydrodynamic entry length. Thermally, fully developed results are obtained when the Nusselt numbers at the inner and outer walls become insensitive to the axial direction along the annulus similar to the cases with no blowing or suction.

Table 2 Results of the heat-transfer analysis with blowing or suction at the walls of the annulus for the fundamental solution of the second kind ($K = 0.5$, $Pr = 0.7$)

Re_i	Re_o	z^+	$Nu_{oo}^{(2)}$	$\theta_{mo}^{(2)}$	$\theta_{oo}^{(2)} - \theta_{mo}^{(2)}$	$\theta_{io}^{(2)} - \theta_{mo}^{(2)}$	$Nu_{ii}^{(2)}$	$\theta_{mi}^{(2)}$	$\theta_{oi}^{(2)} - \theta_{mi}^{(2)}$	$\theta_{ii}^{(2)} - \theta_{mi}^{(2)}$
0.0	0.0	0.0020	11.24	0.0080	0.0890	−0.0080	12.53	0.0040	−0.0040	0.0798
		0.0050	8.040	0.0195	0.1244	−0.0195	9.285	0.0098	−0.0097	0.1077
		0.0075	7.058	0.0291	0.1417	−0.0288	8.288	0.0145	−0.0144	0.1207
		0.0100	6.499	0.0386	0.1539	−0.0376	7.719	0.0193	−0.0189	0.1295
		0.0500	5.087	0.1916	0.1966	−0.0822	6.216	0.0961	−0.0418	0.1609
		0.1000	5.043	0.3828	0.1983	−0.0854	6.166	0.1921	−0.0428	0.1622
		0.5000	5.042	1.9120	0.1983	−0.0854	6.165	0.9597	−0.0429	0.1622
1.0	−1.0	0.0020	10.97	0.0083	0.0911	−0.0083	11.88	0.0043	−0.0043	0.0841
		0.0050	7.814	0.0203	0.1280	−0.0203	8.676	0.0107	−0.0107	0.1153
		0.0075	6.848	0.0303	0.1460	−0.0301	7.693	0.0160	−0.0159	0.1300
		0.0100	6.299	0.0402	0.1587	−0.0393	7.132	0.0214	−0.0209	0.1402
		0.0500	4.848	0.1831	0.2063	−0.0905	5.597	0.0994	−0.0486	0.1787
		0.1000	4.773	0.3306	0.2095	−0.0945	5.515	0.1802	−0.0507	0.1813
		0.5000	4.768	1.0020	0.2097	−0.0948	5.509	0.5492	−0.0508	0.1815
3.0	−3.0	0.0020	10.46	0.0089	0.0955	−0.0089	10.66	0.0050	−0.0050	0.0938
		0.0050	7.384	0.0221	0.1354	−0.0221	7.555	0.0128	−0.0128	0.1324
		0.0075	6.450	0.0329	0.1550	−0.0327	6.612	0.0195	−0.0194	0.1512
		0.0100	5.919	0.0435	0.1689	−0.0427	6.074	0.0261	−0.0256	0.1646
		0.0500	4.418	0.1755	0.2263	−0.1050	4.529	0.1117	−0.0649	0.2208
		0.1000	4.279	0.2846	0.2337	−0.1141	4.385	0.1841	−0.0707	0.2280
		0.5000	4.245	0.6528	0.2356	−0.1166	4.349	0.4292	−0.0722	0.2299
		1.0000	4.244	0.8415	0.2356	−0.1166	4.348	0.5549	−0.0722	0.2299
6.0	−6.0	0.0020	9.755	0.0099	0.1025	−0.0099	9.004	0.0062	−0.0062	0.1111
		0.0050	6.789	0.0249	0.1473	−0.0249	6.107	0.0170	−0.0169	0.1637
		0.0075	5.901	0.0371	0.1695	−0.0370	5.244	0.0261	−0.0261	0.1907
		0.0100	5.395	0.0488	0.1853	−0.0483	4.755	0.0352	−0.0328	0.2103
		0.0500	3.876	0.1753	0.2580	−0.1266	3.299	0.1419	−0.0977	0.3031
		0.1000	3.659	0.2627	0.2732	−0.1457	3.097	0.2198	−0.1133	0.3228
		0.5000	3.533	0.5156	0.2830	−0.1581	2.980	0.4498	−0.1233	0.3355
		1.0000	3.526	0.6354	0.2835	−0.1588	2.974	0.5593	−0.1239	0.3362
		3.0000	3.524	0.8296	0.2837	−0.1590	2.972	0.7369	−0.1241	0.3365
−1.0	1.0	0.0020	11.51	0.0077	0.0869	−0.0077	13.21	0.0037	−0.0037	0.0757
		0.0050	8.273	0.0187	0.1209	−0.0187	9.925	0.0089	−0.0089	0.1007
		0.0075	7.274	0.0279	0.1375	−0.0276	8.919	0.0132	−0.0131	0.1121
		0.0100	6.707	0.0371	0.1491	−0.0360	8.346	0.0175	−0.0171	0.1198
		0.0500	5.344	0.2062	0.1871	−0.0761	6.896	0.0958	−0.0359	0.1450
		0.1000	5.324	0.5078	0.1878	−0.0769	6.873	0.2351	−0.0363	0.1455
−3.0	3.0	0.0020	12.07	0.0072	0.0828	−0.0072	14.62	0.0032	−0.0032	0.0684
		0.0050	8.764	0.0172	0.1141	−0.0171	11.30	0.0074	−0.0074	0.0885
		0.0075	7.731	0.0256	0.1293	−0.0253	10.29	0.0109	−0.0108	0.0972
		0.0100	7.143	0.0343	0.1400	−0.0328	9.723	0.0145	−0.0140	0.1028
		0.0500	5.912	0.3035	0.1691	−0.0621	8.442	0.1244	−0.0263	0.1184

Conclusions

The following conclusions have been made concerning the numerical solution of simultaneously developing velocity and temperature fields in annuli with constant temperatures or heat fluxes with injection or extraction at the walls.

1) With no blowing or suction at the boundaries, the numerical results were in excellent agreement with previous analytical results. The fully developed Nusselt numbers at the walls for the fundamental solutions of the first and second kind are independent of the Prandtl number.

2) The results for injection indicate a negative pressure drop in the direction of flow. For extraction, the pressure drop is also negative. However, for high extraction velocities the pressure increases after an initial drop at the inlet. There is little or no tendency of obtaining fully developed behaviors for suction cases due to complete mass extraction.

3) The injection of a fluid into an annulus decreases the heat transfer at the walls, and the extraction of fluid from the annulus increases the heat transfer at the walls in the axial direction. The Nusselt numbers for the cases with injection or extraction at the walls is strongly dependent on the Prandtl number.

4) The Nusselt numbers for the case of constant heat rates through the walls are greater than the Nusselt numbers for the case of constant wall temperatures with the same injection or extraction radial Reynolds number specification.

Acknowledgment

Funding for this work was provided by the Thermal Energy Group of the Aero Propulsion Laboratory of the Air Force Wright Aeronautical Laboratories under Contract F-33615-81-C-2012. The author would like to thank Scott Thomas for some of the computational work.

References

[1]Reynolds, W. C., Lundberg, R. E., and McCuen, P. A., "Heat Transfer in Annular Passages. General Formulation of the Problem for Arbitrarily Prescribed Wall Temperatures or Heat Flux," *International Journal of Heat and Mass Transfer,* Vol. 6, 1963, pp. 483-493.

[2]Lundberg, R. E., McCuen, P. A., and Reynolds, W. C., "Heat Transfer in Annular Passages. Hydrodynamically Developed Laminar Flow with Arbitrarily Prescribed Wall Temperatures or Heat Flux," *International Journal of Heat and Mass Transfer,* Vol. 6, 1963, pp. 495-529.

[3]Heaton, H. S., Reynolds, W. C., and Kays, W. M., "Heat Transfer in Annular Passages. Simultaneous Development of Velocity and Temperature Fields in Laminar Flow," *International Journal of Heat and Mass Transfer,* Vol. 7, 1964, pp. 763-781.

[4]Kinney, R. B., "Fully Developed Frictional and Heat-Transfer Characteristics of Laminar Flow in Porous Tubes," *International Journal of Heat and Mass Transfer,* Vol. 11, 1968, pp. 1393-1401.

[5]Raithby, G., "Laminar Heat Transfer in the Thermal Entrance Region of Circular Tubes and Two-Dimensional Rectangular Ducts with Wall Suction and Injection," *International Journal of Heat and Mass Transfer,* Vol. 14, 1971, pp. 223-243.

[6]Raithby, G., "Heat Transfer in Tubes and Ducts with Wall Mass Transfer," *Canadian Journal of Engineering,* Vol. 50, 1972, pp. 456-461.

[7]Doughty, J. R. and Perkins, H. C., "The Thermal Entry Problem for Laminar Flow Between Parallel Porous Plates," *Journal of Heat Transfer,* Vol. 93, Nov. 1971, pp. 476-478.

[8]Doughty, J. R. and Perkins, H. C., "Thermal and Combined Entry Problems for Laminar Flow Between Parallel Porous Plates," *Journal of Heat Transfer,* Vol. 94, 1972, pp. 233-234.

[9] Kinney, R. B. and Sparrow, E. M., "Turbulent Flow, Heat Transfer, and Mass Transfer in a Tube with Surface Suction," *Journal of Heat Transfer,* Vol. 92, 1970, pp. 117-125.

[10]Rhee, S. J. and Edwards, D. K., "Laminar Entrance Flow in a Flat Plate Duct with Asymmetrical Suction and Heating," *Numerical Heat Transfer,* Vol. 4, 1981, pp. 85-100.

[11]Faghri, A., "Vapor Flow Analysis in a Double-Walled Concentric Heat Pipe," *Numerical Heat Transfer,* Vol. 10, No. 6, 1986, pp. 583-595.

[12]Faghri, A. and Thomas, S., "Performance Characteristics of a Concentric Annular Heat Pipe: Part I—Experimental Prediction and Analysis of the Capillary Limit," *ASME Proceedings of the 1988 National Heat Transfer Conference,* Vol. 1, 1988, pp. 379-388. Also to appear in *ASME Journal of Heat Transfer.*

[13]Faghri, A., "Performance Characteristics of a Concentric Annular Heat Pipe: Part II—Vapor Flow Analysis," *ASME Proceedings of the 1988 National Heat Transfer Conference,* Vol. 1, 1988, pp. 389-396. Also to appear in *ASME Journal of Heat Transfer.*

[14]Faghri, A. and Parvani, S., "Numerical Analysis of Laminar Flow in a Double-Walled Annular Heat Pipe," *Journal of Thermophysics and Heat Transfer,* Vol. 2, 1988, pp. 165-171.

[15]Kay, W. M. and Crawford, M. E., *Convective Heat and Mass Transfer,* 2nd ed. McGraw-Hill, 1980.